ELSEVIER

Seminars in
NUCLEAR
MEDICINE

Single-Photon Emission Computed Tomography/Computed Tomography: Basic Instrumentation and Innovations

Michael K. O'Connor, PhD, and Brad J. Kemp, PhD

Correlation of the anatomical and functional information presented by single-photon emission computed tomography (SPECT) and computed tomography (CT) can aid in the decision-making process by enabling better localization and definition of organs and lesions and improving the precision of surgical biopsies. Technical developments over the past 20 years have led to the development of better software techniques for image fusion and, more recently, to the development of modern SPECT/CT systems. While image fusion techniques have been in clinical use for many years, the first commercial SPECT/CT system was only developed in 1999. Following the commercial success of PET/CT systems that employed multidetector CT (MDCT) scanners, there has been renewed interest in the development of comparable SPECT/CT systems. This has resulted in the development of a range of SPECT/CT devices varying from a simple CT add-on to a conventional SPECT system that can provide low-dose CT images to a full MDCT scanner integrated with a SPECT system. The advantages of combining SPECT with CT are numerous and are primarily due to the anatomic referencing and the attenuation correction capabilities of CT. Depending on system design, there are varying technical issues surrounding the different SPECT/CT devices, ranging from cost, radiation dose, planning, and siting requirements to system-specific issues such as table sag and CT artifacts due to patient motion. Motion artifacts should be less prevalent with the faster acquisition times of modern scanners, but are still problematic in the thorax and have not yet been fully resolved as they pertain to the use of CT data for cardiac attenuation correction. As this technology matures, we can expect to see a range of SPECT/CT devices available on the market that range from low-dose 1-4 slice inexpensive CT upgrades of conventional SPECT systems, to SPECT systems incorporating 64 or 128 slices CT scanners. The cost of the high-end CT scanners will exceed the cost of the SPECT scanner and hence the justification for such devices will be heavily dependent on clear demonstration of their value in clinical practice.
Semin Nucl Med 36:258-266

In the evaluation of disease, patients often undergo a multitude of imaging procedures that may include computed tomography (CT), magnetic resonance imaging (MRI), ultrasound, and nuclear medicine procedures. Correlation of the anatomical and functional information presented by these different modalities traditionally has been accomplished by a side-by-side comparison of the results from each procedure. Fusion of images from different modalities can aid in the decision making process by enabling better localization and definition of organs and lesions and improving the precision of surgical biopsies. The purpose of this review is to cover the technical developments during the last 20 years that have lead to the development of better techniques for image fusion and in particular to the development of the modern single-photon emission computed tomography (SPECT)/CT systems.

Department of Nuclear Medicine, Mayo Clinic, Rochester, MN.
Address reprint requests to Michael K. O'Connor, PhD, Department of Nuclear Medicine, Charlton 1-225, Mayo Clinic, Rochester, MN 55905. E-mail: mkoconnor@mayo.edu

Software Approach to Image Fusion

Image fusion usually is performed between an anatomical imaging technique such as CT or MRI and a functional imaging technique such as positron emission tomography (PET) or SPECT. Before the introduction of dedicated PET/CT or SPECT/CT systems, considerable work had been done on the development of software algorithms for the coregistration of anatomical and functional images. It is worth briefly reviewing what has been accomplished with these techniques, particularly as we go forward and look at the cost effectiveness of dual-modality systems.

Initial work in the early 1980s focused on brain studies and used special devices, such as face masks, or stereotactic head holders, to facilitate image fusion.[1,2] By the late 1980s, image fusion was being achieved by a variety of

 0001-2998/06/$-see front matter
doi:10.1053/j.semnuclmed.2006.05.005

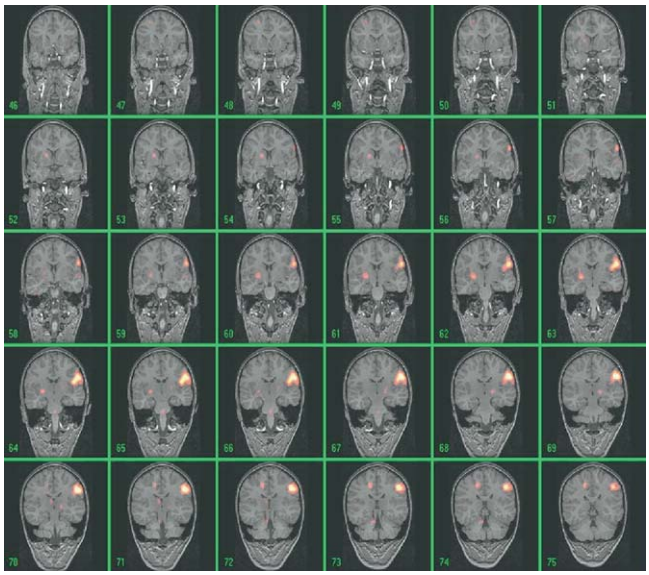

Figure 1 Image coregistration in the detection of epilepsy. Two ^{99m}Tc-HMPAO studies were performed during seizure (ictal) and when the patient was seizure-free (interictal). Both studies and an MR study were coregistered. The differences between the ictal and interictal SPECT studies are superimposed on coronal slices of the MR study to permit accurate localization of the focus of the epilepsy.

software techniques using internal markers.[3-5] During the last 20 years, these algorithms have become more robust and accurate, and current software algorithms permit very accurate coregistration of anatomical and functional images of the brain.[6,7] Figure 1 shows an example of a ^{99m}Tc HMPAO brain SPECT study coregistered to an MR study for the evaluation of epilepsy. This type of image fusion has been a regular component of many clinical practices for several years. However, corresponding techniques for other regions of the body have not achieved the same widespread clinical use.

Image coregistration in the chest or abdomen is considerably more difficult than in the brain for two primary reasons. First, most alignment algorithms rely on the presence of mutual information between the two sets of images, which generally is true of brain studies in which the functional information correlates closely with the anatomical information. However, in the abdomen, the functional image may contain little or no correlative anatomical information, and it is not uncommon to have a functional image show a single focal area of abnormal uptake with no adjacent functional reference points that can be correlated to anatomical reference points. Such highly dissimilar datasets make it difficult for any coregistration algorithm to succeed. Second, the chest and abdomen are not rigid structures and differences in patient positioning and respiratory motion make it difficult to align the anatomical and functional images. One of the most problematic areas is the head and neck, where differences in arm and shoulder positions make coregistration very difficult. Additional problems include differences in shape and curvature of imaging tables, with consequential differences in the shape of the patient. The greater the time interval between the anatomical and functional study, the greater the likelihood for other factors, such as uncontrollable movement of internal organs, bowel contents, and bowel gas, to influence the accuracy of image fusion.

Despite these technical obstacles, a considerable body of work has been conducted on this problem.[8-11] Image registration algorithms can be broadly divided into two groups: those that are feature based (ie, based on alignment of common anatomical landmarks) or volume based (ie, based on iterative algorithms that seek to maximize the measures of similarity between images).[12] More recently newer feature-based and volume-based algorithms have used 3-dimensional elastic transformations and nonlinear warping to improve the accuracy of these fusion techniques.[12] Current results indicate that the accuracy to which the anatomical and functional images (that have been acquired on different imaging systems) can be coregistered in the abdomen and pelvis is approximately 5 to 7 mm.[8,13] Cost considerations and the limited number of integrated SPECT/CT devices in clinical use to date means that work is likely to continue in this area for several years to come. Even with the increased use of dedicated SPECT/CT devices, such software algorithms will still play an important role in accurately correcting for minor mis-registrations due to patient motion, breathing artifacts, etc. In addition there are likely to be situations where the anatomical modality of choice is MR rather than CT and the need will remain for accurate software algorithms to coregister the MR and SPECT or PET images.

Development of SPECT/CT Devices

Much of the early work on the development of a combined SPECT/CT unit was performed at University of California, San Francisco, by Dr Hasegawa and colleagues. Their initial work was focused on the development of a system that could perform simultaneous CT and SPECT studies. Figure 2 shows a schematic diagram of their first system, which used an array of high-purity germanium detectors to simultaneously detect 40 to 100 keV x-rays from an external source and 140 keV gamma rays from an internally administered source.[14,15] The initial goal of this work was to explore the possibility of using the x-ray data to perform attenuation correction of the SPECT data and to provide better region of interest definition for quantification of radiopharmaceutical uptake in a lesion. Because of the 3- to 4-h image acquisition time and the need to rotate the object being scanned, this system was only suitable for animal and phantom studies. However, this work was important because it highlighted, for the first time, the potential benefits of a single device capable of performing anatomical and functional imaging. They demonstrated that such a system was capable of performing attenuation correction and could permit accurate quantification of radiotracer activity in a porcine myocardium.[16] This group was also the first to build a combined SPECT/CT system for clinical studies.[17] This system used a single-slice CT scanner and a single-head large field of view gamma camera (Fig. 3) and was the forerunner of today's systems that combine a multidetector row CT (MDCT) system and dual-detector SPECT system.

The first commercial SPECT/CT system was the GE Hawkeye system (GE Healthcare, Haifa, Israel), which was developed in 1999.[18] This system took

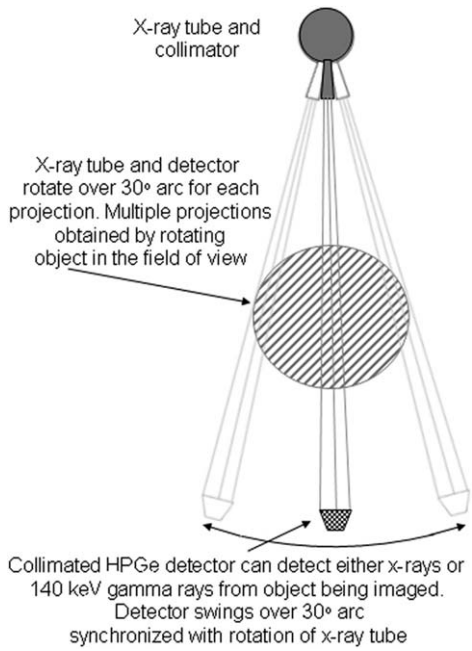

Figure 2 Schematic diagram of the SPECT/CT system developed at UCSF. The system acquires one projection (either SPECT or CT) by rotating the small detector array over a 30° arc. The object being imaged is then rotated for the next projection.

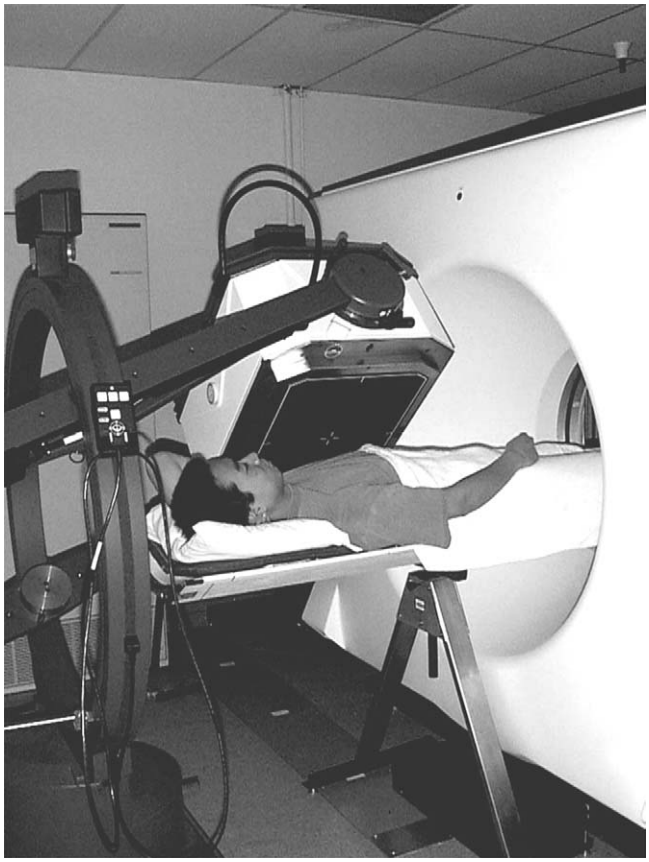

Figure 3 Clinical SPECT/CT system developed at USCF. A conventional single-head gamma camera was positioned at the back of a GE 9800 CT scanner. The CT table could travel through the CT gantry to the SPECT system, thereby allowing SPECT and CT acquisitions of the patient in one examination. (Reprinted with permission from "Dual-Modality Imaging of Cancer with SPECT/CT," Tech Can Res Treat 1:449-458, 2002. Adenine Press, www.tcrt.org.)

advantage of the unique slip-ring gantry of this system to mount an x-ray tube emitting a fan-beam of radiation and an array of 384 Cadmium Tungstate detectors on opposite sides of the slip ring gantry (Fig. 4). Although the slip-ring gantry permitted continuous rotation for the x-ray acquisition, mechanical constraints placed by the heavy detectors limited the rotational speed to ~22 s/orbit. For a transaxial slice, the CT device acquired information over an arc of 213° (180° + fan angle), which took approximately 13 seconds. Each slice had an in-plane resolution of 1.2 mm and an axial thickness of 10 mm. The x-ray system operated at 140 kVp with a tube current of only 2.5 mA. Although this resulted in a significantly lower patient dose (by a factor of 4-5) than what would be delivered using a conventional CT scanner, the quality of the CT images were inferior to state of the art CT scanners both because of the low radiation dose and to the poor axial resolution. However, it should be noted that the primary purpose of this device was not image fusion but rather the production of a high-quality attenuation map for use with the emission data. In this respect, the CT system provided significantly higher-quality attenuation maps than those available with conventional Gd-153 scanning lines sources. The slow scan speed was advantageous in this respect in that breath holding was not possible and the CT images were blurred by respiratory and cardiac motion in a comparable manner to the SPECT raw data.

Following the commercial success of PET/CT systems that use MDCT scanners, there has been renewed interest in the development of comparable SPECT/CT systems. This interest has resulted in the development of two types of SPECT/CT devices, each with their own advantages and disadvantages. GE Healthcare has developed an enhanced version of the Hawkeye system called the Hawkeye-4, which uses the same gantry as the original Hawkeye system but now acquires 4 × 5 mm thick slices with each rotation instead of one 10-mm slice. This design retains the very compact design of the Hawkeye system, delivers a low radiation dose to the patient and requires minimal room shielding.

Two vendors have opted for the development of SPECT/CT systems that are more comparable to their PET/CT counterparts, with the goal of providing high-quality CT images fused to the SPECT image data. The Precedence system (Fig. 5) from Philips Medical Systems (Milpitas, CA) couples a conventional 6-slice or 16-slice CT scanner to their dual-detector Skylight system. The Symbia system (Siemens Medical Solutions, Hoffman Estates, IL) incorporates a 1-, 2-, or 6-slice CT scanner with their dual-detector E-Cam system (Fig. 6). With both systems, CT slice thickness is variable and can be adjusted from 0.6 mm up to 10 mm. The scan speed for a 40-cm axial field of view is less than 30 s. By comparison, the CT scan time on the GE Hawkeye-4 system is 5 min for a 40 cm field of view. However, because of the addition of a separate CT gantry, both the Symbia and Precedence systems are considerably larger than conventional SPECT systems and as discussed below, have very different siting requirements and shielding requirements compared with the GE Hawkeye system.

Technical Aspects of SPECT/CT Imaging

The advantages of combining SPECT with CT are numerous and are primarily due to the anatomic referencing and the attenuation correction capabilities of CT. Whether the CT component that is used in the combined imaging approach should be a conventional MDCT scanner or the more compact, low current CT add-on used on the GE Hawkeye system is currently a matter of debate.

CT Technology

CT technology has undergone a bewildering number of improvements during the last 5 to 10 years[19] with the advent of helical CT and MDCT. Helical or spiral CT represents a volumetric scan with the patient being scanned continuously in the longitudinal direction.[20,21] Helical CT involves the constant motion of the bed as the x-ray tube is rotating around the patient. In effect the focus of the x-ray tube follows a helical trajectory, relative to the patient, as multiple rotations are completed. The slip ring is the enabling technology of helical CT.

MDCT offers the ability to acquire more than one slice simultaneously. The advantages and benefits of MDCT are shorter scan times, extended scan ranges, and improved longitudinal resolution.[22] With MDCT of, for example, 6 slices the operator has several options: scan a given volume 6-times

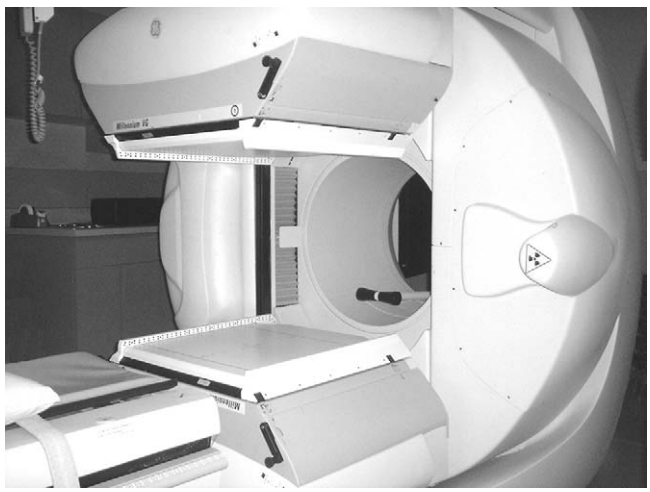

Figure 4 GE Hawkeye system. The first commercial SPECT/CT system developed in 1999. The x-ray tube housing is seen on the right side of the gantry with the array of detectors on the left side.

Figure 5 Phillips Precedence system which combines the Phillips Skylight dual-head gamma camera system with a MDCT system (Courtesy of Phillips, Milpitas, CA).

faster (assuming all other parameters are unchanged); scan a volume that greater by a factor of 6 within the same scan time; or maintain the same scan time and volume but acquire thinner slices. As MDCT systems use wider detector arrays and the number of slices increases the x-ray beam can no longer be considered a fan-beam and special cone-beam reconstruction software is required. A system with greater than four detector rows is generally considered as cone beam.

A large number of factors determine the noise, low contrast resolution and high contrast (spatial) resolution of the CT image. Noise, in simplest terms, is measured as the standard deviation of voxel values in a homogeneous (typically water) phantom. Noise is influenced by tube current (mA), voltage (kVp), exposure time, table speed, slice thickness, reconstruction algorithm, and filter kernel. Noise is primarily determined by the number of x-rays passing through the body—a higher tube current and/or exposure time reduces the noise, but at the expense of higher patient dose. An increase in the tube current by a factor of N will reduce the noise by $N^{1/2}$ but will result in an N-fold increase in dose.

Low-contrast resolution is the ability of the system to resolve objects having a small difference from background. Low contrast resolution is determined by the same factors that affect noise. A doubling of the slice thickness increases contrast resolution by the same factor, although with a loss in axial resolution. Faster gantry rotation speed increases noise, as most CT systems have an upper limit on the x-ray tube current. Spatial resolution is determined primarily by the system geometric resolution limits (such as the size of the focal spot and detector elements), slice thickness, pixel size and reconstruction filter.

The most common CT artifacts are patient motion, beam hardening, and partial volume. Motion artifacts should be less prevalent with the faster acquisition times of modern scanners, but are still problematic in the thorax.

Beam hardening is the preferential absorption of lower energy x-rays as the x-ray beam passes through an attenuating medium. As a result, the mean energy of the x-ray beam increases (hardens) as the attenuation increases. The CT scanner is calibrated to correct for beam hardening in tissue equivalent attenuators.[23] Two-pass beam-hardening corrections can be used for scans (such as a head scan) in which the attenuation characteristics deviate significantly from those of water.[24,25] Beam hardening manifests itself as a cupping artifact in a uniform attenuator, because the object appears less attenuating than in actuality, and can manifest itself as dark streaks between high attenuating structures; for example between the petrous bones in the base of the skull.

A third less-common problem is partial volume averaging, whereby a variety of different tissues are contained within one slice. With the modern MDCT scanners, thinner slices, the ability to reconstruct slices at arbitrary locations and the ability to rebin the slice data have helped to minimize this problem.

Of the current SPECT/CT systems, the GE Hawkeye, uses a modified 3rd-generation technology with an x-ray tube and detector array that rotate in synchrony. This type of technology requires that the array of detectors be accurately balanced as each detector gives rise to an annulus of image information. If a detector becomes miscalibrated, the data from that detector can generate a ring artifact in the reconstructed image. This is somewhat comparable to nonuniformity in the uniformity map of a SPECT camera resulting in a ring artifact in the transaxial data.

Scatter is an artifact that has become more important as the axial extent of detectors has increased. Hence it becomes more of an issue for the Siemens Symbia and Philips Precedence systems, which use 7th-generation CT technology. The detection of scattered radiation can cause a cupping artifact in which the CT numbers are reduced; the inclusion of scatter makes the object appear less attenuating.[26,27] To reduce the amount of scattered radiation, septa are positioned between the detectors and aligned with the x-ray tube to mechanically reject scatter. The total scatter is about 4% for single and 4-slice systems. MDCT is more susceptible to the detection of scattered x-rays than single slice CT. In MDCT the x-rays can scatter and still strike a detector. Scatter correction is difficult in CT because the detectors do not operate in photon counting mode (so the energy of the detected radiograph is not measured) and the beam is polychromatic so the system does not know the original energy of the scattered x-ray.

Attenuation Correction

To correct SPECT images for attenuation the spatial distribution of attenuation coefficients within the patient must be known. This attenuation map is then incorporated into a statistically based, iterative reconstruction algorithm such as ordered subset expectation maximization (ie, OSEM).[28,29] During the 1990s much research and development was undertaken designing transmission imaging systems that used a radionuclide source of photons and the SPECT camera as the detector; the most common transmission imaging system used a scanning line source.[30-32]

The spatial distribution of attenuation coefficients also can be measured

Figure 6 Siemens Symbia system. This is an integrated gantry that contains a MDCT system and the dual-detector E-Cam system (Courtesy of Siemens Medical Systems, Hoffman Estates, IL).

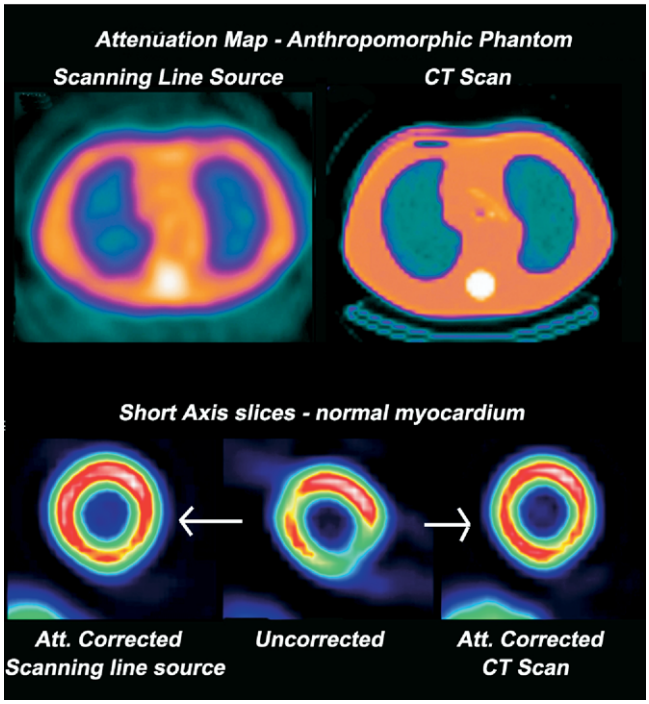

Figure 7 Attenuation maps of an anthropomorphic phantom containing a normal myocardium generated using a Gd-153 line source and a CT scan. Midventricular short axis slices show that application of both attenuation correction maps yield comparable results, indicating that high resolution per se is not a requirement for accurate attenuation correction.

using a CT scanner. With any type of CT system, the image noise in attenuation maps will be very low, and the in-plane resolution will be high compared with maps generated from radionuclide-based transmission systems. Although CT systems generate a higher resolution map, the improvement in resolution is not necessarily a factor in the accuracy of the attenuation compensation because we are primarily concerned with obtaining an accurate estimate of the attenuation path length for each pixel in the SPECT transaxial data. Figure 7 shows examples of attenuation maps of an anthropomorphic phantom generated using the GE Hawkeye device and the GE MG dual-head gamma camera system equipped with a ^{153}Gd scanning line source. The phantom contained a "normal" myocardium and attenuation compensation was performed using identical software algorithms on the two systems, thereby allowing one to determine the impact of the differences in the resolution and fidelity of the attenuation map on image quality. As seen in Figure 7, both maps adequately correct for the attenuation defect in the inferior wall of the myocardium and no significant difference was observed in the quality of the attenuation corrected images produced by these different maps.

Although both CT and the radionuclide-based transmission systems can produce effective attenuation maps under ideal conditions, they have significantly different advantages and limitations. There are 4 primary benefits of using CT images for attenuation correction of SPECT data: the CT image has less noise than transmission images acquired using radionuclide sources; the CT image can be acquired faster than a transmission image; the CT acquisition has a high flux and hence the CT images will not be influenced by cross-talk from the SPECT radionuclide; and the CT source does not decay.

The precision and noise in the attenuation corrected SPECT images are dependent on the emission and transmission statistics. Noise in the transmission images—and in the attenuation coefficients—propagate into the attenuation-corrected SPECT images. Tung and Gullberg[33] showed that with an efficient, radionuclide-based transmission system the statistical noise in the attenuation corrected SPECT images was dominated by the emission statistics. This is because the correction uses the line integral of attenuation coefficients so the effect of noise in individual pixels is minimized.[30] However, the attenuation coefficients derived from the transmission images experience increased bias and noise as the source decays; consequently the sources must be replaced frequently to maintain adequate transmission statistics to minimize noise propagation and to ensure emission contamination does not overwhelm the transmission counts.[34] In addition, algorithms must be employed with radionuclide-based transmission systems to remove the cross-contamination between the emission and transmission photons.[35] With CT systems, the x-ray flux is orders of magnitude greater than the emission count rate so cross-talk is not an issue. As such, the CT scan can be acquired after the patient is injected with the radiopharmaceutical without concern of the emission photons contaminating the transmission data.

An advantage of radionuclide based transmission systems is that they usually employ simultaneous acquisition of the emission and transmission data, thereby eliminating any misregistration between the SPECT data and the attenuation maps. SPECT/CT systems, on the other hand, acquire SPECT and CT data sequentially and the potential for patient movement and misregistration exists. The sources of misregistration and their effects are discussed below.

Derivation of Attenuation Coefficients

In order for the CT image to be used in the attenuation correction algorithm, the CT numbers (in Hounsfield units, HU) must be converted to attenuation coefficients at the energy of the SPECT radionuclide. Attenuation is dependent on the energy of the x-rays and the conversion of a CT image into an attenuation map requires an assumed effective energy of the polychromatic x-ray beam. This effective energy of the x-ray spectrum depends on the kVp, the x-ray beam filtration, and beam hardening within the patient.

The conversion of the CT image into an attenuation map can be done by segmentation, scaling, or a hybrid technique.[36] In segmentation the CT image is divided into regions of different tissue types such as bone, soft tissue and lung, and a fixed value of the attenuation coefficient for the energy of the radionuclide is assigned to those regions. This approach may work well for dissimilar tissues, but it can introduce errors at tissue boundaries where the change in tissue type is not discontinuous. Further, the segmentation technique can introduce errors if the patient specific value differs from that assigned by the algorithm. For example, the attenuation coefficient in lung can differ by 30%[37] and in bone it can vary depending on the relative proportion of cortical and trabecular bone.[38]

The simplest scaling method uses linear scaling based on the attenuation coefficients of water at the CT and SPECT energies.[39,40] Specifically, the attenuation coefficients are estimated by multiplying the CT numbers by the ratio of the water attenuation coefficients at the SPECT and CT energies. This method works well for tissue whose attenuation is primarily Compton scatter but it is not effective in tissue of high atomic number where the photoelectric absorption is a greater component of attenuation. The scaling method can also use a bilinear curve to multiplicatively scale the measured CT numbers. This approach models tissue with an HU of −1000 to 0 as a mixture of soft tissue and air, and tissue with an HU greater than 0 is modeled as a mixture of soft tissue and bone.[41-43] Nickoloff and coworkers[44] used constant scale factors for both soft tissue and bone. The hybrid method is similar to the bilinear scaling approach in that two mixtures of tissue are modeled. Segmentation is used to divide the CT image into bone and nonbone regions and a separate scaling is then used for each region.[36]

There are other issues concerning the conversion of the CT image to an attenuation map. The CT images have better resolution than their SPECT counterparts. Hence, the CT images need to be down-sampled to the matrix size of the SPECT images and reduced in resolution[43,45] to reduce the inclusion of artifacts into the SPECT data. Application of these conversion algorithms in PET/CT have shown that the attenuation coefficients will have negligible noise but may have bias.[46,47]

Sources of Error

There are several sources of error in the application of SPECT/CT, depending on the system configuration. These errors include misregistration, truncation, scatter, and beam hardening artifacts. A major issue for CT type systems

is misregistration between the emission and transmission data, resulting in incorrect matching of the attenuation map to the emission data.[48] This may occur for a number of reasons, including sagging of the emission table, respiratory and cardiac motion, and patient motion. With the 1st-generation SPECT/CT systems (GE Hawkeye system), the CT and SPECT components were not designed as an integrated unit. The SPECT table was merely advanced axially from the gamma camera detector to the CT detector. Because this step involved increasing or decreasing the length of table suspended in air, the flex of the table could change resulting in misalignment between the SPECT and CT images. Misregistration was a significant problem, affecting approximately 20% of clinical studies on the original GE Hawkeye design.[48] The impact of misregistration on the emission scans is highly patient dependent. Artifacts can occur with a misalignment of as little as 1 pixel (~7 mm) in the y-direction (ventral to dorsal direction), which can superimpose parts of the myocardium over lung tissue. This can result in underestimation of attenuation path length in this part of the myocardium and under-corrected of the emission scan that can lead to the creation of apical or anterior wall defects in the attenuation compensated images (Fig. 8).

Recent upgrades to the support arm and rollers of the imaging table on this type of system have helped minimize sagging and poor tracking of the imaging table on these 1st-generation systems. Figure 9 shows the effect of table sagging on the registration of the emission and transmission images in a series of patients undergoing rest and stress myocardial perfusion imaging.[49] Results are shown both before and after an upgrade to the support rollers guiding the table top. These problems should be minimal on many of the newer generation of SPECT/CT systems as these employ a dual-table configuration. In this configuration, the patient pallet is generally a low attenuation carbon fiber tabletop that sits on top of a second, more rigid, lower table. The carbon fiber tabletop can be suspended in air from the lower table, to permit the patient to be imaged over 360° with the SPECT system. The rigid lower table is then used to move the patient in the axial direction between the CT and SPECT sections of the scanner. Hence the degree of flex of the upper table is not altered during the procedure. This eliminates table problems although it does not insure that the patient will not move between procedures.

Respiratory and cardiac motions are most problematic with the faster CT scanners. Because the CT component is now a MDCT unit capable of high speed rotation, it can acquire anywhere from 2 to 16 slices per step. Acquisition time per slice can be as short as 200 to 300 milliseconds. For a cardiac study the CT component is usually acquired in 30 seconds with the patient

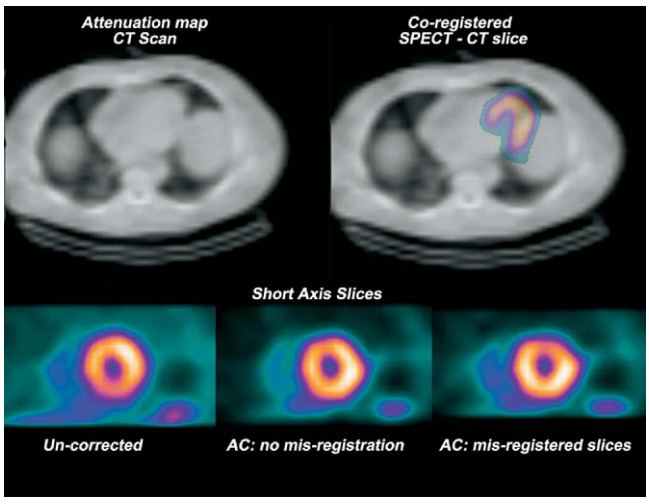

Figure 8 Top row shows the CT-generated attenuation map and the fused SPECT/CT slices in a myocardial perfusion study. Note that part of the myocardium appears to overlap the lung region. Bottom row shows the uncorrected and attenuation corrected short axis slices. Note the artifactual apical defect in the attenuation correction slice that was eliminated after re-alignment of the SPECT and CT data.

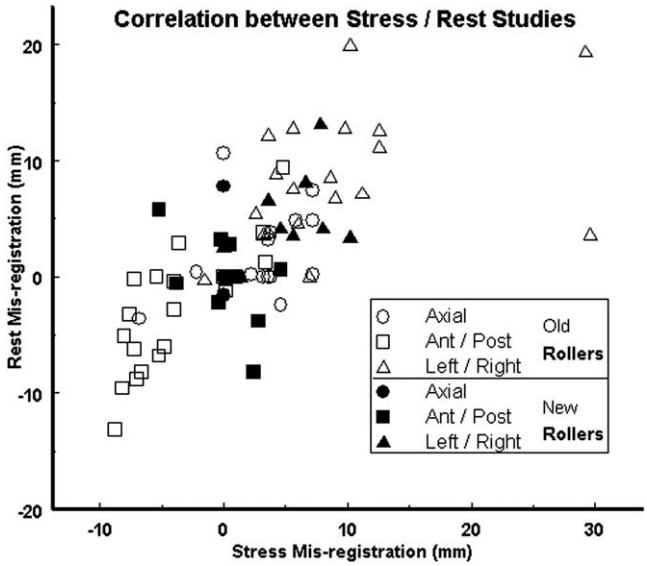

Figure 9 Degree of misregistration noted on rest and stress myocardial perfusion studies before and after installation of an improved roller system to reduce table sagging. Head, post and left refer to inferior/superior, anterior/posterior and left/right shifts respectively.

breathing normally. Hence images of the thorax represent a snap-shot at fixed points in the patient's respiratory and cardiac cycles. The SPECT component, on the other hand, typically takes 15 to 20 minutes and the images represent an average of the respiratory and cardiac cycles. These 2 independent motions can be a major source of error and will need to be addressed before the full benefits of these faster CT systems can be seen for cardiac applications.

These problems are similar to those encountered in PET/CT systems. Current studies indicate that, in PET cardiac studies, the use of radionuclide-based transmission imaging may be preferable to CT-generated attenuation maps. Chin and coworkers[50] found that, in clinical PET/CT studies, misregistration of the diaphragm between the CT and PET data is associated with relative decreased emission activity in inferior, inferoseptal, and inferolateral walls and recommended further studies to determine whether the frequency of these findings warrants the use of ^{68}Ge transmission attenuation correction in myocardial ^{18}F-fluorodeoxyglucose (FDG) PET. Dorbala and coworkers[51] found that a post-stress CT scan reduced the misregistration error of the attenuation map in Rb-82 PET myocardial perfusion images. Out of 66 patients studied only 6% of cases had misregistration with a late, post-stress CT scan versus 42% with a CT scan acquired at peak hyperemia. The implementation of a slow CT scan to minimize respiration artifacts in cardiac PET has also been proposed.[52]

A variety of methods have been proposed to minimize the registration error. In PET/CT, some laboratories recommend acquiring the CT scan during shallow breathing or recommend that the patient hold their breath at mid-expiration or mid-inspiration. Both techniques do not completely eliminate breathing artifact.[53-55] Shallow breathing results in blurring of the CT images, whereas breath holding can be more difficult with respect to patient compliance, particularly in a patient population with severe illness and poor physical condition. Beyer and coworkers[56] found that there were fewer propensities for artifact in those protocols in which the patient breathed normally and the CT scanner possessed at least 6 detector rows. Pan and coworkers[57] found that 50% of patients undergoing a whole-body PET/CT study with midexpiration breath-hold had misalignment between PET and CT and in 34% of the studies this misalignment was greater than 2 cm. However, by acquiring a respiratory gated CT study and averaging the time bins these errors could be markedly reduced.[57]

Given this information, it is important that the SPECT/CT system use a coregistration program and associated QC phantom on a daily basis to insure correct alignment between the SPECT and CT scanners (see "Anatomic

Referencing"). In addition, in cases in which patient motion corrupts the alignment, it is important that the system have a QC program that allows the user to re-align the SPECT and CT image sets either manually or through a semiautomated program.

Truncation of parts of the torso can result in underestimation of the attenuation path length and can lead to corruption of the attenuation corrected emission studies. Current low-dose CT devices (Hawkeye, Hawkeye-4) have an x-ray field of view of ~40 cm and hence are unable to adequately image patients with a chest circumference of greater than 55 cm. Figure 10 shows the effects of truncation of the CT attenuation map on reconstructed image quality. Mild truncation at the shoulders does not have a major impact on image quality, as it does not seriously corrupt the estimate of the attenuation path length for pixels in the myocardium. However with increasing truncation, the attenuation path lengths are underestimated resulting in under-correction of the emission images. Current SPECT/CT devices using a conventional MDCT scanner have a larger (50 cm) field of view and hence less issues with patient truncation, although even these may not be able to adequately image the ever increasing number of obese patients.

Although no extensive large scale clinical studies have been reported on the value of SPECT/CT devices in attenuation correction, preliminary studies in patients have reported some discrepancies between attenuation compensated myocardial perfusion studies using CT and Gd-153 transmission sources and have highlighted the problems of noise and mis-registration between the CT and SPECT images that are discussed above.[58-60]

Anatomic Referencing

Coregistration of anatomy and function is less dependent on the fidelity of the CT image than the attenuation correction algorithm. However, the accurate coregistration of the SPECT and CT data are just as important as with attenuation correction, and many of the pitfalls discussed previously, vis-à-vis table sagging, patient motion, and respiratory and cardiac motion, all apply equally to image fusion. Most vendors now include a calibration procedure to insure that, in the absence of patient-related artifacts, both the CT and SPECT images are correctly coregistered in 3 dimensions. Figure 11 shows the calibration jig used on the GE Hawkeye-4 system. A series of 6 syringes containing an appropriate radionuclide are inserted into a foam calibration jig so that they are orientated in 3 orthogonal planes. The calibration jig is positioned mid-table and 10 to 15 kg is placed at the end of the table to simulate table flex with a patient. After SPECT/CT acquisition, software automatically determines the location of the syringes and either computes the necessary calibration factors to insure precise alignment of the CT and SPECT images, or on a routine basis, confirms the validity of the existing calibration factors. This type of calibration procedure is essential if the clinician is to have confidence in the ability of the technology to permit accurate localization of radiotracer uptake in the body.

The use of contrast enhancement in CT is currently being studied for PET/CT procedures to see if there is added benefit in anatomical localization of tumors.[61] Unmodified adaptation of CT contrast protocols into PET/CT can potentially introduce artifacts into the PET images when the CT images

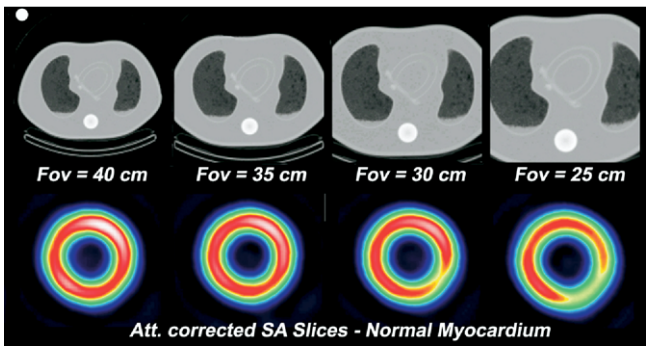

Figure 10 Effect of changes in the x-ray field of view from 40 cm to 25 cm on the attenuation corrected short axis slices of a normal myocardium in an anthropomorphic phantom.

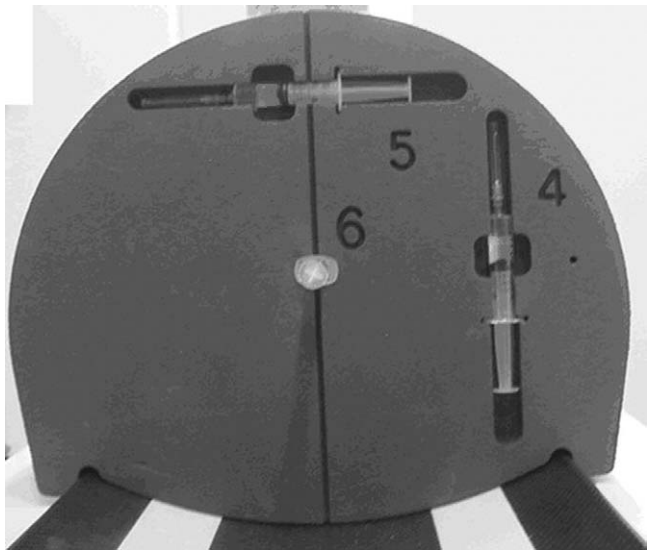

Figure 11 Calibration jig employed on the GE Hawkeye-4 system. The foam jig contains 6 syringes (3 of which can be seen in the photograph) oriented along 3 axes. When imaged on both the SPECT and CT systems they permit accurate alignment between the CT and SPECT data (Courtesy of GE Health care, Haifa, Israel).

are used for attenuation correction.[62] Several studies have demonstrated the need for changes in the contrast injection techniques and/or use of water-based oral contrast agents.[63,64] If use of contrast material in PET/CT becomes routine clinical practice, it would be expected to likewise extend into SPECT/CT procedures. Its use in SPECT/CT may be less problematic than in PET/CT as attenuation correction is not routinely performed on many SPECT/CT procedures. Where contrast enhancement is seen as beneficial, its application may be restricted to SPECT/CT devices with conventional MDCT capability to provide the temporal resolution needed to image the contrast material.

Planning/Siting Requirements for SPECT/CT

The space required for a SPECT/CT system depends on the type of system being installed. The GE Hawkeye or GE Hawkeye-4 only requires the same room size as conventional SPECT systems. Minimum room size for these types of units is typically 14′ × 16′. Because of the x-ray tube on these systems, some lead shielding of the room is required. The exposure rate from these systems is approximately 20 times less than that from a conventional MDCT scanner. Hence lead shielding in the walls is usually only required for that portion of the wall closest to the x-ray tube. Figure 12 shows a typical room layout for a GE Hawkeye system and the exposure rate and regions requiring shielding for an installation of this type of system. In addition, if the operator console is located at the end of the imaging table, the exposure rate is low enough that no separate control booth is required.

For SPECT/CT systems using a MDCT scanner, a larger room is required (a minimum of 15′ × 24′), along with a separate control booth. Typically at least 1/16-inch lead shielding (4 lbs/ft^2) or equivalent is required for the walls, doors, floors, ceilings, and operator's barrier. The concrete equivalence of 1/16-inch thick lead would be about 4 to 6 inches of standard-density concrete (147 pounds per cubic foot). SPECT/CT rooms with high workloads and with fully occupied uncontrolled space directly adjacent to the scanner may need shielding that is thicker than 1/16-inch lead or 4 to 6 inches of concrete to meet the recommended NCRP Report #147 shielding design goal of 0.02 mGy per week (1 mGy per year) for persons in uncontrolled areas.[65]

One additional factor to be considered in siting these instruments is the weight-bearing capability of the floor. The GE Hawkeye unit has a gantry weight of approximately 5,500 lbs whereas the Siemens Symbia and Philips

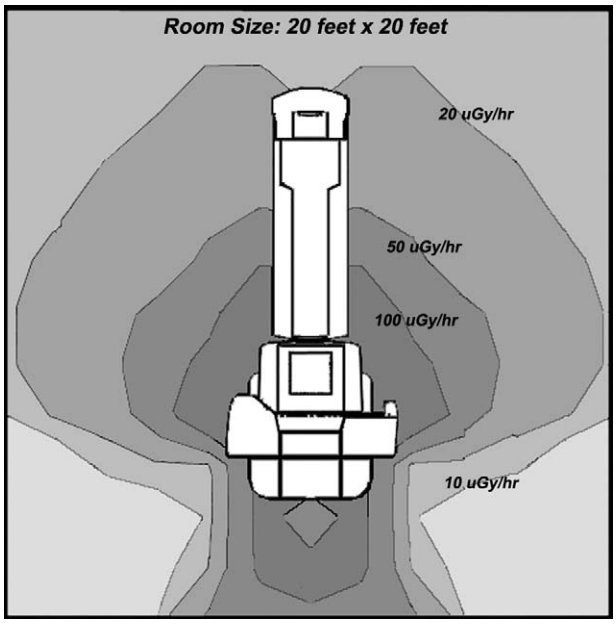

Figure 12 Typical room layout for a low-mA SPECT/CT system (GE Hawkeye). Isodose contour levels are shown. Shielding (1/16-inch lead) is usually required at the walls along the sides and back of the gantry.

Precedence units have gantry weights of approximately 8,000 lbs and approximately 10,000 lbs, respectively. These weight limits should be kept in mind during the planning phase of new installations.

Future Applications and Advances for SPECT/CT Technology

In addition to attenuation correction and co-registration, other possible applications for this emerging technology include patient dosimetry and radiotherapy. The development of more-sophisticated co-registration applications should permit estimation of organ or tumor volume from the anatomical data rather than the emission data. Traditional calculations of organ and tumor size from emission data are problematic, particularly for small tumors in which the limited spatial resolution of SPECT can introduce significant errors into volume estimates. The use of the CT data for volume estimation should permit more accurate quantification of tumor uptake of radiopharmaceuticals for therapy applications.

There are a number of intriguing applications for this technology in cardiology including quantifying coronary artery calcium, evaluating the patency of vascular and coronary arteries, and assessing myocardial perfusion and viability in one clinical setting. While the current generation of SPECT/CT devices is not capable of imaging the coronary arteries, it is technically possible to integrate the new faster 64-slice CT scanners into a SPECT/CT device. While such a device would be very expensive, it may yield additional clinical benefits not possible from separate SPECT and CT examinations.

In an ideal world, the SPECT/CT system should consist of one detector that can simultaneously detect the gamma emissions from the patient and the x-ray emissions from the CT system. Conventional nuclear medicine technology is count-rate limited to the degree that would not permit this type of system. However semiconductor detectors utilizing materials such as Cadmium-Zinc-Telluride have been used for both x-ray and nuclear studies[66,67] and these devices can be operated in both current mode (for x-ray studies), or individual event mode for nuclear studies.

As this technology matures, we can expect to see a range of SPECT/CT devices become available on the market that range from low dose 1- to 4-slice inexpensive CT upgrades to conventional SPECT systems, to SPECT systems incorporating 64- or 128-slice CT scanners. The cost of the high-end CT scanners will exceed the cost of the SPECT scanner and hence the justification for such devices will be heavily dependent on clear demonstration of their value in the clinical practice.

References

1. Bergstrom M, Boethius J, Eriksson L, et al: Head fixation device for reproducible positron alignment in transmission CT and positron emission tomography. J Comput Assis Tomogr 5:136-141, 1981
2. Bettinardi V, Scardaoni R, Gilardi MC, et al: Head holder for PET, CT and MR studies. J Comput Assist Tomogr 15:886-892, 1991
3. Woods RP, Cherry SR, Mazziotta JC: Rapid automated algorithm for aligning and reslicing PET images. J Comput Assist Tomogr 16:620-633, 1992
4. Pietrzyk U, Herholz K, Fink G, et al: An interactive technique for three-dimensional image registration: validation for PET, SPECT, MRI and CT brain studies. J Nucl Med 35:2011-2018, 1994
5. Pelizzari CA, Chen GTY, Spelbring DR, et al: Accurate three-dimensional registration of CT, PET and/or MR images of the brain. J Comput Assist Tomogr 13:20-26, 1989
6. Wiest R, Kassubek J, Schindler K, et al: Comparison of voxel-based 3-D MRI analysis and subtraction ictal SPECT coregistered to MRI in focal epilepsy. Epilepsy Res 65:125-33, 2005
7. Cascino GD, Buchhalter JR, Mullan BP, et al: Ictal SPECT in nonlesional extratemporal epilepsy. Epilepsia 45:32-34, 2004 (Suppl 4)
8. Perault C, Schvartz C, Wampach H, et al: Thoracic and abdominal SPECT-CT image fusion without external markers in endocrine carcinomas. J Nucl Med 38:1234-1242, 1997
9. Scott AM, Macapinlac H, Zhang J, et al: Image registration of SPECT and CT images using an external fiduciary band and three-dimensional surface fitting in metastatic thyroid cancer. J Nucl Med 36:100-103, 1995
10. Yu JN, Fahey FH, Gage HD, et al: Intermodality, retrospective image registration in the thorax. J Nucl Med 36:2333-2338, 1995
11. Goerres GW, Kamel E, Heidelberg T-NH, et al: PET-CT image co-registration in the thorax: influence of respiration. Eur J Nucl Med 29:351-360, 2002
12. Slomka PJ: Software approach to merging molecular with anatomic information. J Nucl Med 45:36S-45S, 2004 (Suppl 1)
13. Forster GJ, Laumann C, Nickel O, et al: SPET/CT image co-registration in the abdomen with a simple and cost-effective tool. Eur J Nucl Med 30:32-39, 2003
14. Hasagawa BH, Stebler B, Rutt BK, et al: A prototype high-purity germanium detector system with fast photon counting circuitry for medical imaging. Med Phys 18:900-999, 1991
15. Lang TF, Hasagawa BH, Liew SC, et al: Description of a prototype emission-transmission CT imaging system. J Nucl Med 33:1881-1887, 1992
16. Khali K, Blankespoor SC, Brown JK, et al: Myocardial perfusion imaging with a combined x-ray CT and SPECT system. J Nucl Med 38:1535-1540, 1997
17. Tang HR, Da Silva AJ, Matthay KK, et al: Neuroblastoma imaging using a combined CT scanner – scintillation camera and ^{131}I- MIBG. J Nucl Med 42:237-247, 2001
18. Bocher M, Balan A, Krausz Y, et al: Gamma camera-mounted anatomical x-ray tomography: technology, system characteristics and first images. J Nucl Med 27:619-627, 2000
19. Kohl G: The evolution and state-of-the-art principles of multislice computed tomography. Proc Am Thorac Soc 2:470-476, 2005
20. Kalender WA, Seissler W, Klotz E, et al: Spiral volumetric CT with single-breath-hold technique, continuous transport, and continuous scanner rotation. Radiology 176:181-183, 1990
21. Crawford CR, King KF: Computed tomographic scanning with simultaneous patient translation. Med Phys 17:967-982, 1990
22. Flohr TG, Schaller S, Stierstorfer K, et al: Multi-detector row CT systems and image reconstruction techniques. Radiology 235:756-773, 2005
23. Joseph PM, Spital RD: A method for correcting bone induced artifacts

in computed tomography scanners. J Comput Assist Tomogr 2:100-108, 1978
24. Yan CH, Whalen RT, Beaupre GS, et al: Reconstruction algorithm for polychromatic CT imaging: application to beam hardening correction. IEEE Trans Med Imaging 19:1-11, 2000
25. Joseph PM, Ruth C: A method for simultaneous correction of spectrum hardening artifacts in CT images containing both bone and iodine. Med Phys 24:1629-1634, 1997
26. Glover GH: Compton scatter effects in CT reconstructions. Med Phys 9;860-867, 1982.
27. Joseph PM, Spital RD: The effects of scatter in x-ray computed tomography. Med Phys 9:464-472, 1982
28. King MA, Tsui BMW, Pan TS, et al: Attenuation compensation for cardiac single-photon emission computed tomographic imaging: part 2: Attenuation compensation algorithms. J Nucl Cardiol 3:55-63, 1996
29. Hutton BF, Hudson HM, Beekman FJ: A clinical perspective of accelerated statistical reconstruction. Eur J Nucl Med 24:797-808, 1997
30. King MA, Tsui BMW, Pan TS: Attenuation compensation for cardiac single-photon emission computed tomographic imaging: part 1. Impact of attenuation and methods of estimating attenuation maps. J Nucl Cardiol 2:513-524, 1995
31. Gullberg GT: Innovative design concepts for transmission CT in attenuation-corrected SPECT imaging. J Nucl Med 39:1344-1347, 1998
32. Zaidi H, Hasegawa B: Determination of the attenuation map in emission tomography. J Nucl Med 44:291-315, 2003
33. Tung CH, Gullberg GT: A simulation of emission and transmission noise propagation in cardiac SPECT imaging with nonuniform attenuation correction. Med Phys 21:1565-1576, 1994
34. Almquist H, Arheden H, Arvidsson AH, et al: Clinical implication of down-scatter in attenuation-corrected myocardial SPECT. J Nucl Cardiol 6:406-411, 1999
35. Jaszczak RJ, Gilland DR, Hanson MW, et al: Fast transmission CT for determining attenuation maps using a collimated line source, rotatable air-copper-lead attenuators and fan-beam collimation. J Nucl Med 34: 1577-1586, 1993
36. Kinahan PE, Townsend DW, Beyer T, et al: Attenuation correction for a combined 3D PET/CT scanner. Med Phys 25:2046-2053, 1998
37. van Dyk J, Keane TJ, Rider WD: Lung density as measured by computerized tomography: implications for radiotherapy. Int J Radiat Oncol Biol Phys 8:1363-1372, 1982
38. Woodard HQ, White DR: Bone models for use in radiotherapy dosimetry. Br J Radiol 55:277-282, 1982
39. Fleming JS: A technique for using CT images in attenuation correction and quantification in SPECT. Nucl Med Commun 10:83-97, 1989
40. LaCroix KJ, Tsui BMW, Hasegawa BH, et al: Investigation of the use of X-ray CT images for attenuation compensation in SPECT. IEEE Trans Nucl Sci 41:2793-2799, 1994
41. Blankespoor SC, Wu X, Kalki JK, et al: Attenuation correction of SPECT using x-ray CT on an emission-transmission CT system: myocardial perfusion assessment. IEEE Trans Nucl Sci 43:2263-2274, 1996
42. Bai C, Shao L, Da Silva AJ, et al: A generalized model for the conversion from CT numbers to linear attenuation coefficients. IEEE Trans Nucl Sci 50:1510-1515, 2003
43. Burger C, Goerres G, Schoenes S, et al: PET attenuation coefficients from CT images: experimental evaluation of the transformation of CT into PET 511-keV attenuation coefficients. Eur J Nucl Med Mol Imaging 7:922-927, 2002
44. Nickoloff EL, Perman WH, Esser PD, et al: Left ventricular volume: physical basis for attenuation correction in radionuclide determinations. Radiology 152:511-515, 1984
45. Meikle SR, Dahlbom M, Cherry SR: Attenuation correction using count-limited transmission data in positron emission tomography. J Nucl Med 34:143-150, 1993
46. Nakamoto Y, Osman M, Cohade C, et al: PET/CT: comparison of quantitative tracer uptake between germanium and CT transmission attenuation-corrected images. J Nucl Med 43:1137-1143, 2002
47. Kamel E, Hany TF, Burger C, et al: CT vs 68Ge attenuation correction in a combined PET/CT system: evaluation of the effect of lowering the CT tube current. Eur J Nucl Med Mol Imaging 29:346-350, 2002
48. Fricke H, Fricke E, Weise R, et al: A method to remove artifacts in attenuation-corrected myocardial perfusion spect introduced by misalignment between emission scan and ct-derived attenuation maps. J Nucl Med 45:1619-1625, 2004
49. Ruter RL, O'Connor MK: Effect of table support on the accuracy of the alignment between the SPECT and CT images in myocardial perfusion studies on a GE Hawkeye system. J Nucl Med Technol 33:107-108, 2005 (abstract)
50. Chin BB, Nakamoto Y, Kraitchman DL, et al: PET-CT evaluation of 2-deoxy-2-[18F] fluoro-D-glucose myocardial uptake: effect of respiratory motion. Mol Imaging Biol 5:57-64, 2003
51. Dorbala S, Limaye A, Sampson U, et al: Optimal timing of transmission map for Rubidium-82 stress positron emission tomography myocardial perfusion imaging. (abstract). J Nucl Med 46:267P, 2005
52. DiFilippo FP, Brunken RC, Neumann DR, et al: Cardiac positron emission tomography using a slow CT for attenuation correction. (abstract). Mol Imaging Biol 6:86, 2004
53. Osman MM, Cohade C, Nakamoto Y, et al: Respiratory motion artifacts on PET emission images obtained using CT attenuation correction on PET-CT. Eur J Nuc Med Mol Imaging 30:603-606, 2003
54. Cohade C, Osman M, Marshall LN, et al: PET-CT: accuracy of PET and CT spatial registration of lung lesions. Eur J Nuc Med Mol Imaging 30:721-726, 2003
55. von Schulthess GK: Normal PET and PET/CT body scans: imaging pitfalls and artifacts, in von-Schulthess GK, ed: Clinical Molecular Anatomic Imaging: PET, PET/CT and SPECT/CT. Baltimore, MD: Lippincott, Williams and Wilkins pp 252-270, 2002
56. Beyer T, Rosenbaum S, Veit P, et al: Respiration artifacts in whole-body (18)F-FDG PET/CT studies with combined PET/CT tomographs employing spiral CT technology with 1 to 16 detector. Eur J Nucl Med Mol Imaging 32:1429-1439, 2005
57. Pan T, Mawlawi O, Nehmeh SA, et al: Attenuation correction of PET images with respiration-averaged CT images in PET/CT. J Nucl Med 46:1481-1487, 2005
58. Kjaer A, Cortsen A, Federspiel M, et al: Comparison of attenuation correction in myocardial SPECT using gadolinium-153 line source or low-dose CT. (abstract). Eur J Nucl Med 31:S318, 2004 (suppl 2)
59. Namdar M, Siegrist PT, Koepfli P, et al: CT-Attenuation correction in myocardial perfusion SPECT using a hybrid SPECT/CT. (abstract). Eur J Nucl Med 31 Suppl 2:S261, 2004 (suppl 2)
60. Halama JR, Henkin RE, Sajdak RA, et al: X-Ray CT registration requirements for attenuation correction in myocardial perfusion SPECT. (abstract). J Nucl Med 45:417P, 2004
61. Reza Ay M, Zaidi H: Assessment of errors caused by X-ray scatter and use of contrast medium when using CT-based attenuation correction in PET. Eur J Nucl Med Mol Imaging, in press
62. Antoch G, Freudenberg LS, Beyer T, et al: To enhance or not to enhance? F18-FDG and CT contrast agents in dual-modality F18-FDG PET/CT. J Nucl Med 45:56S-65S, 2004 (suppl 1)
63. Beyer T, Antoch G, Bockisch A, et al: Optimized intravenous contrast administration for diagnostic whole-body F18-FDG PET/CT. J Nucl Med 46:429-435, 2005
64. Antoch G, Kuehl H, Kanja J, et al: Introduction and evaluation of a negative oral contrast agent to avoid contrast-induced artefacts in dual modality PET/CT imaging. Radiology 230:879-885, 2004
65. National Counsel on Radiation Protecton: Structural Shielding Design for Medical X-ray Imaging Facilities, NCRP Report No. 147, National Council on Radiation Protection and Measurement. Bethesda, MD, NCRP, 2004
66. Zeng GL, Gagnon D: Image reconstruction algorithm for a spinning strip CZT SPECT camera with a parallel slat collimator and small pixels. Med Phys 31:3461-3473, 2004
67. Miyajima S, Imagawa K: CdZnTe detector in mammographic x-ray spectroscopy. Phys Med Biol 47:3959-3972, 2002